Hindawi Publishing Corporation
Journal of Nanomaterials
Volume 2015, Article ID 175605, 5 pages
http://dx.doi.org/10.1155/2015/175605

Research Article

Growth of $BiFeO_3$ Microcylinders under a Hydrothermal Condition

L. J. Di,[1] H. Yang,[1,2] T. Xian,[1] J. Y. Ma,[2] H. M. Zhang,[1] J. L. Jiang,[1] Z. Q. Wei,[1] and W. J. Feng[1]

[1]*School of Science, Lanzhou University of Technology, Lanzhou 730050, China*
[2]*State Key Laboratory of Advanced Processing and Recycling of Non-Ferrous Metals, Lanzhou University of Technology, Lanzhou 730050, China*

Correspondence should be addressed to H. Yang; hyang@lut.cn

Received 22 April 2014; Revised 26 September 2014; Accepted 26 September 2014

Academic Editor: Debasis Dhak

Copyright © 2015 L. J. Di et al. This is an open access article distributed under the Creative Commons Attribution License, which permits unrestricted use, distribution, and reproduction in any medium, provided the original work is properly cited.

$BiFeO_3$ microcylinders were synthesized via a hydrothermal condition. SEM observation reveals that with increasing the hydrothermal reaction time from 6 to 15 h, the microcylinders grow from ~0.7 to ~4.1 μm in height, whereas their diameter remains to be 3.7-3.8 μm with a minor change. The microcylinders are mainly made up of sphere-like grains of 100–150 nm in size. A possible growth mechanism of the $BiFeO_3$ microcylinders is proposed. The photocatalytic activity of the as-prepared $BiFeO_3$ samples was evaluated by the degradation of acid orange 7 under simulated sunlight irradiation, revealing that they possess an appreciable photocatalytic activity. Magnetic hysteresis loop measurement shows that the $BiFeO_3$ microcylinders exhibit a typical antiferromagnetic behavior at room temperature.

1. Introduction

Bismuth ferrite ($BiFeO_3$) with a rhombohedrally distorted perovskite structure has been extensively studied as one of single-phase multiferroic materials in the past few years [1, 2]. $BiFeO_3$ exhibits ferroelectricity with a Curie temperature (T_C) of ~830°C and antiferromagnetism with a Néel temperature (T_N) of ~380°C, making it a promising candidate for room-temperature multiferroic applications [3, 4]. Furthermore, $BiFeO_3$ is an important semiconductor with bandgap energy of about 2.2 eV and has a pronounced photocatalytic activity for the degradation of various organic dyes under visible-light irradiation [5–11]. Generally, the physical and chemical properties of a functional material depend highly on its morphologies, dimensions, sizes, defects, and so forth. To tailor or enhance the properties of the material, it is especially interesting to create nano/microstructures with various morphologies. Up to now, a large number of nano/microstructures of $BiFeO_3$ have been synthesized including microplatelets, microcubes, nanotubes, nanofibers, microflowers, microspheres, microrods, thick film, microoctahedron, and nanoparticles [5–19]. Various wet chemical methods have been widely used to achieve those nano/microstructures of $BiFeO_3$. Among them, the hydrothermal route has special advantages in tailoring the product morphology. The variation of any parameter in the hydrothermal reaction process, such as reaction temperature and time, mineralizer type and its concentration, pH value, metal ion concentration, and organic additive, could result in morphologically different products. In this work, we report the synthesis of $BiFeO_3$ microcylinders under a hydrothermal route and a possible growth mechanism of the microcylinders is proposed. The photocatalytic activity of as-prepared samples was evaluated by the degradation of acid orange 7 (AO7) under simulated sunlight irradiation.

2. Experimental

0.005 mol of $Bi(NO_3)_3{\cdot}5H_2O$ and 0.005 mol of $Fe(NO_3)_3{\cdot}9H_2O$ were dissolved in 20 mL of dilute nitric acid solution. Then to the mixture solution was added 60 mL KOH solution with a concentration of 9 mol·L^{-1} drop by drop under magnetic stirring, and immediately a dark

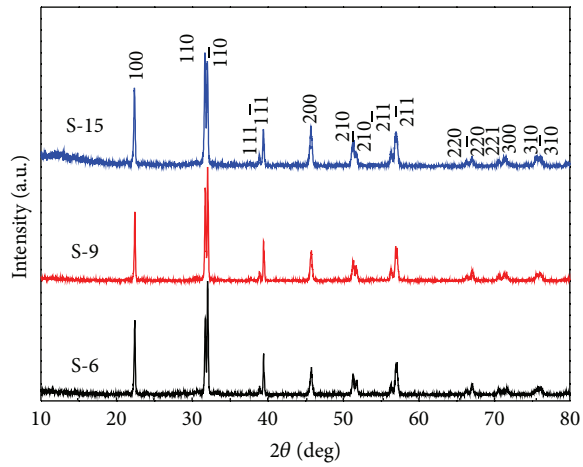

FIGURE 1: XRD patterns of $BiFeO_3$ samples prepared at the reaction time of 6, 9, and 15 h (the corresponding samples are termed S-6, S-9, and S-15, resp.).

brown suspension solution was formed. The suspension was ultrasonically treated for 8 min and subsequently stirred vigorously with a magnetic stirrer for 30 min to create a highly uniform mixture. The resulted mixture was sealed in a Teflon-lined stainless steel autoclave of 100 mL capacity and submitted to hydrothermal treatment at 200°C. After different reaction time, the autoclave was cooled naturally to room temperature. The resulting brown precipitate was collected and washed several times with distilled water and absolute ethanol and then dried in a thermostat drying oven at 80°C for 12 h to obtain final $BiFeO_3$ product. By varying the reaction time from 6 to 15 h, several $BiFeO_3$ samples were prepared.

The phase purity of the samples was examined by means of X-ray powder diffraction (XRD) with Cu Kα radiation. The morphology of the samples was observed by field-emission scanning electron microscope (SEM). The ultraviolet- (UV-) visible diffuse reflectance spectra were measured using a UV-visible spectrophotometer with an integrating sphere attachment. A vibrating sample magnetometer (VSM) was used to measure the magnetic hysteresis loops of the samples at room temperature.

The photocatalytic activity of the products was evaluated by degrading AO7 in aqueous solution under simulated sunlight irradiation from a 200 W xenon lamp. The initial AO7 concentration was 5 mg·L^{-1} and the $BiFeO_3$ loading was 0.1 g in 200 mL of AO7 solution. Before illumination, the mixed solution was ultrasonically treated for 15 min in the dark to make $BiFeO_3$ particles uniformly dispersed. During the photocatalysis process, the water-jacketed reactor was cooled with water-cooling system to keep the solution at room temperature. After irradiation for 8 h, the reaction solution was centrifuged for 10 min at 3000 r·min^{-1} to remove $BiFeO_3$ particles. The AO7 concentration was determined by measuring the absorbance of the solution at a fixed wavelength of 484 nm using an UV-visible spectrophotometer. The percentage degradation is defined as $(C_0 - C_t)/C_0 \times 100\%$, where C_0 and C_t are the AO7 concentrations before and after irradiation, respectively.

3. Results and Discussion

Figure 1 shows the XRD patterns of $BiFeO_3$ samples prepared at the reaction time of 6, 9, and 15 h (the corresponding samples are termed S-6, S-9, and S-15, resp.). For these samples, all the diffraction peaks can be indexed in terms of the rhombohedral structure of $BiFeO_3$ with space group *R3m* (PDF card number 74-2016). No traces of other phases are detected in the XRD patterns, revealing high purity of the as-prepared products. The widths of the diffraction peaks undergo no obvious change between the samples, indicating that they have nearly the same grain or subgrain size.

Figure 2 shows the SEM images of the as-prepared $BiFeO_3$ samples, revealing the synthesis of cylinder-like microparticles. When the hydrothermal reaction time is 6 h, the resulting sample consists of microcylinders with an average diameter of ~3.7 μm and height of ~0.7 μm (Figure 2(a)). When the reaction time is increased to 9 h, the obtained microcylinders have a diameter of ~3.8 μm and height of ~1.7 μm (Figure 2(b)). Further prolonging of the reaction time up to 15 h leads to the formation of microcylinders with a diameter of ~3.8 μm and height of ~4.1 μm (Figure 2(c)). This implies the continuous growth of $BiFeO_3$ microcylinders along the direction of height with increasing the reaction time, whereas their diameter undergoes minor change. Figure 2(d) shows an enlarged view of the SEM image of Figure 2(b), revealing that the microcylinders are mainly made up of sphere-like grains of 100–150 nm in size.

Figure 3 shows a possible growth mechanism of the cylinder-like $BiFeO_3$ particles. Initially, Bi^{3+} and Fe^{3+} ions react with OH^- ions to produce amorphous $Bi(OH)_3$ and $Fe(OH)_3$ precipitates, and then the hydroxides undergo an attack of the mineralizer, KOH, to dissolve and form ion groups. These species undergo nucleation and growth when critical supersaturation is reached, leading to the formation of $BiFeO_3$ nanocrystals. The nascent nanocrystals come together or self-assemble to form cylinder-like aggregates. This self-organization process can be understood according to the oriented-attachment growth mechanism, where the

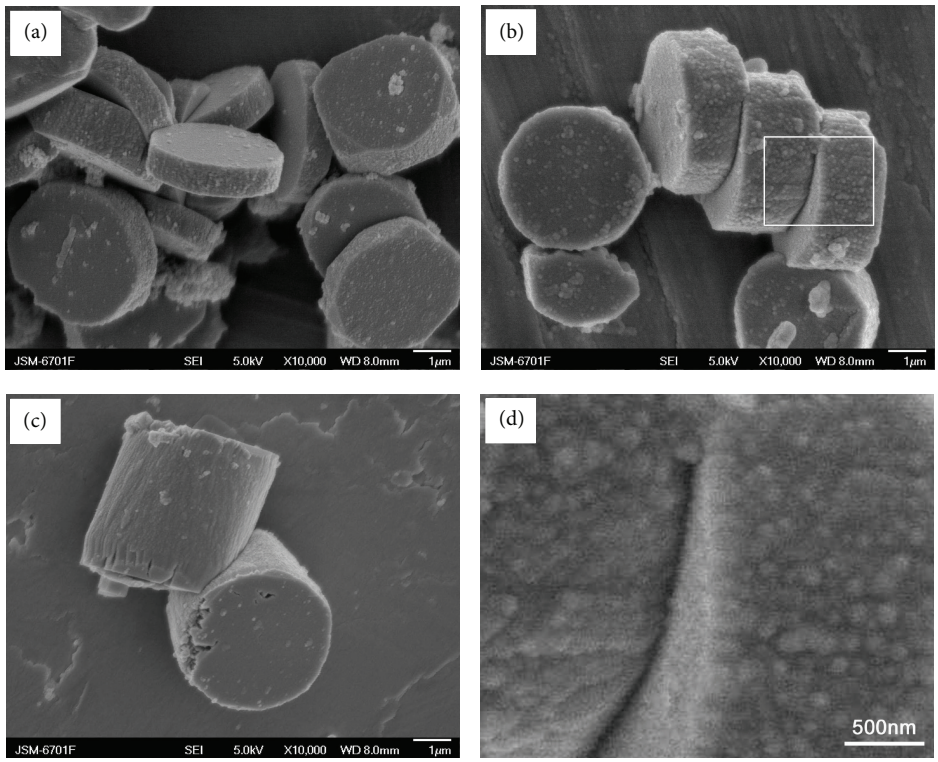

Figure 2: SEM images of $BiFeO_3$ samples. (a) S-6, (b) S-9, (c) S-15, and (d) enlarged image of sample S-9.

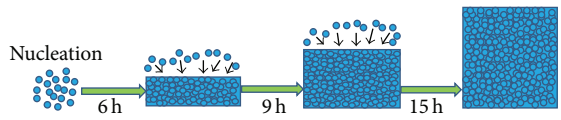

Figure 3: Schematic illustration of the growth mechanism for cylinder-like $BiFeO_3$ particles.

driving force is the reduction of overall surface energy [20, 21]. At the initial stage of the self-organization, thin or disk-like microcylinders with a diameter of about 3.7-3.8 μm are constructed from $BiFeO_3$ nanocrystals. With increasing the reaction time, $BiFeO_3$ nanocrystals are continuously attracted to attach on the surface of the microcylinders, leading to their continuous growth along the height direction, whereas their diameter undergoes minor change.

Figure 4(a) shows the UV-visible diffuse reflectance spectra of $BiFeO_3$ samples and Figure 4(b) gives the corresponding first derivative of the reflectance (R) with respect to wavelength λ (i.e., $dR/d\lambda$). It is seen that the samples have a similar absorption edge at ~568 nm, which is assigned to the electron transition from valence band to conduction band according to the theoretical results [22]. From the absorption edge, the bandgap energy of the samples is obtained to be 2.18 eV.

Figure 5 shows the photocatalytic degradation of AO7 over $BiFeO_3$ samples as a function of irradiation time (t), along with the blank experimental result. AO7 appears to be stable under simulated sunlight irradiation in the absence of photocatalyst, and its degradation percentage is less than 7% after 8 h of exposure. When $BiFeO_3$ samples are used as the photocatalyst, the degradation of AO7 is obviously enhanced, indicating an appreciable photocatalytic activity of the samples. The degradation percentage of AO7 after 8 h irradiation with samples S-6, S-9, and S-15 is about 56%, 28%, and 19%, respectively. The sample S-6 exhibits the highest photocatalytic activity, which is mainly ascribed to its relatively small particle size. Generally small particle size and large surface area to volume ratio is required to achieve good photocatalytic activity since the photocatalytic reaction occurs dominantly on the catalyst surface [23].

Figure 6 shows the magnetic hysteresis loops of $BiFeO_3$ samples measured at room temperature, revealing a nearly linear dependence of the magnetization on applied magnetic field. This indicates that all the samples exhibit an antiferromagnetic behavior at room temperature. It is well known that $BiFeO_3$ has a helical antiferromagnetic spin structure with a period of ~62 nm [24]. This helimagnetic structure will be destroyed in nanosized $BiFeO_3$, making the spin compensation incomplete. As a result, weak ferromagnetism is generally observed for nanosized $BiFeO_3$ and exhibits an increasing trend with reducing the grain size [10, 25].

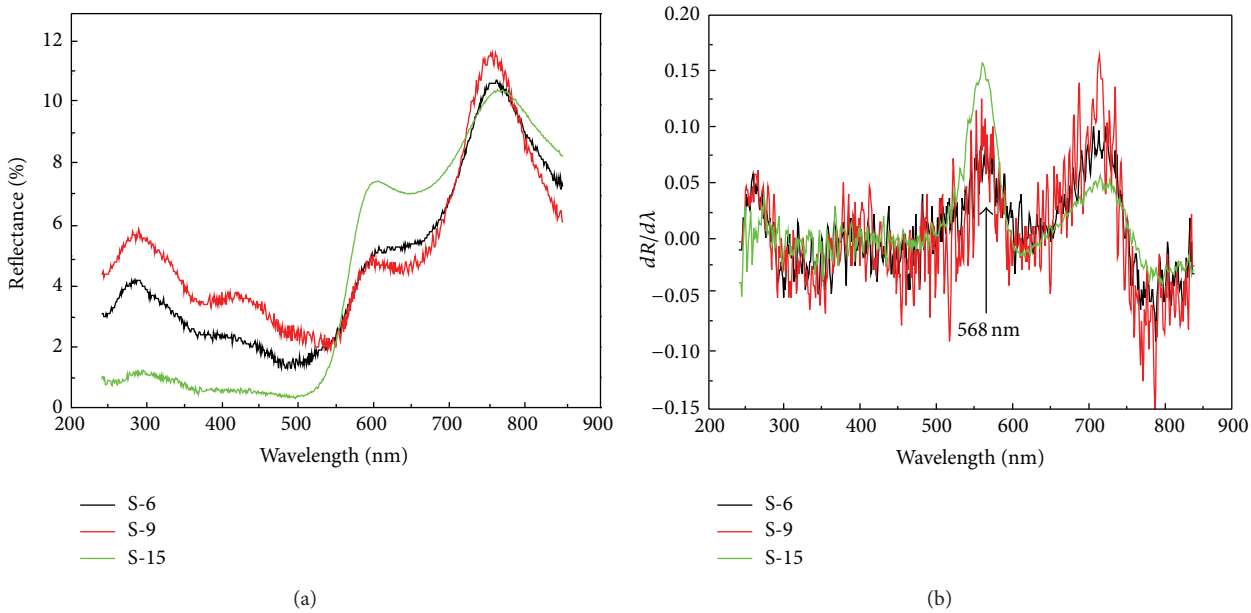

FIGURE 4: (a) UV-visible diffuse reflectance spectra of $BiFeO_3$ samples and (b) the corresponding first derivative of the diffuse reflectance spectra.

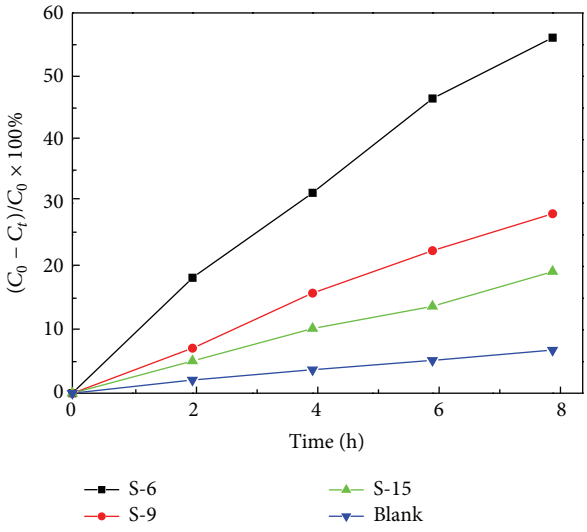

FIGURE 5: Photocatalytic degradation of AO7 over $BiFeO_3$ samples as a function of irradiation time along with the blank experiment result.

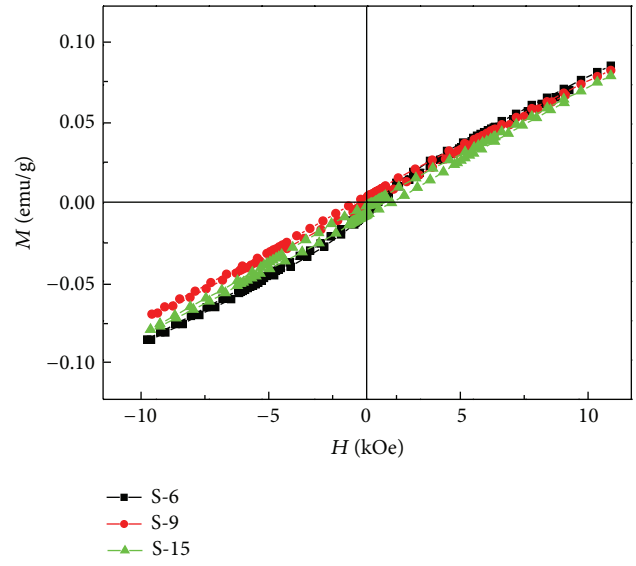

FIGURE 6: Magnetic hysteresis loops of $BiFeO_3$ samples measured at room temperature.

However, $BiFeO_3$ samples synthesized in this work crystallize in relatively large-sized microcrystals, which inhibits the observation of macroscopic magnetization.

4. Conclusions

Cylinder-like $BiFeO_3$ particles were successfully prepared by a hydrothermal method. It is found that the height of the resulted $BiFeO_3$ microcylinders has a dependence on the hydrothermal reaction time. With prolonging the reaction time from 6 to 15 h, the height of the microcylinders increases from ~0.7 to ~4.1 μm, whereas their diameter undergoes a minor change (3.7-3.8 μm). The microcylinders are constructed from sphere-like $BiFeO_3$ nanocrystals of 100–150 nm in size. Photocatalytic experimental results demonstrate that the $BiFeO_3$ microcylinders exhibit an appreciable photocatalytic activity toward the degradation of AO7 under simulated sunlight irradiation. Magnetic hysteresis loop measurement reveals an antiferromagnetic behavior in the $BiFeO_3$ microcylinders at room temperature.

Conflict of Interests

The authors declare that there is no conflict of interests regarding the publication of this paper.

Acknowledgments

This work was supported by the National Natural Science Foundation of China (Grant nos. 51262018 and 11264023) and the Hongliu Outstanding Talents Foundation of Lanzhou University of Technology (Grant no. J201205).

References

[1] J. Wang, J. B. Neaton, H. Zheng et al., "Epitaxial $BiFeO_3$ multiferroic thin film heterostructures," *Science*, vol. 299, no. 5613, pp. 1719–1722, 2003.

[2] M. Fiebig, T. Lottermoser, D. Fröhlich, A. V. Goltsev, and R. V. Pisarev, "Observation of coupled magnetic and electric domains," *Nature*, vol. 419, no. 24, pp. 818–820, 2002.

[3] C. Tabares-Munoz, J. P. Rivera, A. Monnier, and H. Schmid, "Measurement of the quadratic magnetoelectric effect on single crystalline $BiFeO_3$," *Japanese Journal Physics of Applied Physics*, vol. 24, no. 2, pp. 1051–1053, 1985.

[4] P. Fischer, M. Polomska, I. Sosnowska, and M. Szymanski, "Temperature dependence of the crystal and magnetic structures of $BiFeO_3$," *Journal of Physics C: Solid State Physics*, vol. 13, no. 10, pp. 1931–1940, 1980.

[5] X. Lǔ, J. Xie, Y. Song, and J. Lin, "Surfactant-assisted hydrothermal preparation of submicrometer-sized two-dimensional $BiFeO_3$ plates and their photocatalytic activity," *Journal of Materials Science*, vol. 42, no. 16, pp. 6824–6827, 2007.

[6] T. Soltani and M. H. Entezari, "Photolysis and photocatalysis of methylene blue by ferrite bismuth nanoparticles under sunlight irradiation," *Journal of Molecular Catalysis A: Chemical*, vol. 377, pp. 197–203, 2013.

[7] J. Wei, C. Zhang, and Z. Xu, "Low-temperature hydrothermal synthesis of $BiFeO_3$ microcrystals and their visible-light photocatalytic activity," *Materials Research Bulletin*, vol. 47, no. 11, pp. 3513–3517, 2012.

[8] X. Yang, Y. Zhang, G. Xu et al., "Phase and morphology evolution of bismuth ferrites via hydrothermal reaction route," *Materials Research Bulletin*, vol. 48, no. 4, pp. 1694–1699, 2013.

[9] S. Mohan and B. Subramanian, "A strategy to fabricate bismuth ferrite ($BiFeO_3$) nanotubes from electrospun nanofibers and their solar light-driven photocatalytic properties," *RSC Advances*, vol. 3, no. 45, pp. 23737–23744, 2013.

[10] X. Zhang, H. Liu, B. Zheng, Y. Lin, D. Liu, and C.-W. Nan, "Photocatalytic and magnetic behaviors observed in $BiFeO_3$ nanofibers by electrospinning," *Journal of Nanomaterials*, vol. 2013, Article ID 917948, 7 pages, 2013.

[11] T. Xian, H. Yang, J. F. Dai, Z. Q. Wei, J. Y. Ma, and W. J. Feng, "Photocatalytic properties of $BiFeO_3$ nanoparticles with different sizes," *Materials Letters*, vol. 65, no. 11, pp. 1573–1575, 2011.

[12] X. Chen, Y. Tang, L. Fang, H. Zhang, C. Hu, and H. Zhou, "Self-assembly growth of flower-like $BiFeO_3$ powders at low temperature," *Journal of Materials Science: Materials in Electronics*, vol. 23, no. 8, pp. 1500–1503, 2012.

[13] H. Zheng, X. Liu, C. Diao, Y. Gu, and W. Zhang, "A separation mechanism of photogenerated charges and magnetic properties for $BiFeO_3$ microspheres synthesized by a facile hydrothermal method," *Physical Chemistry Chemical Physics*, vol. 14, no. 23, pp. 8376–8381, 2012.

[14] L. Zhang, X.-F. Cao, Y.-L. Ma, X.-T. Chen, and Z.-L. Xue, "Polymer-directed synthesis and magnetic property of nanoparticles-assembled $BiFeO_3$ microrods," *Journal of Solid State Chemistry*, vol. 183, no. 8, pp. 1761–1766, 2010.

[15] H.-Y. Si, W.-L. Lu, J.-S. Chen, G.-M. Chow, X. Sun, and J. Zhao, "Hydrothermal epitaxial multiferroic $BiFeO_3$ thick film by addition of the PVA," *Journal of Alloys and Compounds*, vol. 577, no. 15, pp. 44–48, 2013.

[16] L. J. Di, H. Yang, T. Xian, R. S. Li, Y. C. Feng, and W. J. Feng, "Influence of precursor Bi^{3+}/Fe^{3+} ion concentration on hydrothermal synthesis of $BiFeO_3$ crystallites," *Ceramics International*, vol. 40, no. 3, pp. 4575–4578, 2014.

[17] M. Muneeswaran, P. Jegatheesan, and N. V. Giridharan, "Synthesis of nanosized $BiFeO_3$ powders by co-precipitation method," *Journal of Experimental Nanoscience*, vol. 8, no. 3, pp. 341–346, 2013.

[18] A. Perejón, N. Murafa, P. E. Sánchez-Jiménez et al., "Direct mechanosynthesis of pure $BiFeO_3$ perovskite nanoparticles: reaction mechanism," *Journal of Materials Chemistry C*, vol. 1, no. 22, pp. 3551–3562, 2013.

[19] A. Hernández-Ramírez, A. Martínez-Luévanos, A. F. Fuentes, A.-G. D. Nelson, R. C. Ewing, and S. M. Montemayor, "Molten salts activated by high-energy milling: a useful, low-temperature route for the synthesis of multiferroic compounds," *Journal of Alloys and Compounds*, vol. 584, no. 25, pp. 93–100, 2014.

[20] R. L. Penn, G. Oskam, T. J. Strathmann, P. C. Searson, A. T. Stone, and D. R. Veblen, "Epitaxial assembly in aged colloids," *The Journal of Physical Chemistry B*, vol. 105, no. 11, pp. 2177–2182, 2001.

[21] R. L. Penn and J. F. Banfield, "Imperfect oriented attachment: dislocation generation in defect-free nanocrystals," *Science*, vol. 281, no. 5379, pp. 969–971, 1998.

[22] S. J. Clark and J. Robertson, "Band gap and Schottky barrier heights of multiferroic $BiFeO_3$," *Applied Physics Letters*, vol. 90, no. 1–3, Article ID 132903, 2007.

[23] Z. Zhang, C.-C. Wang, R. Zakaria, and J. Y. Ying, "Role of particle size in nanocrystalline TiO_2-based photocatalysts," *Journal of Physical Chemistry B*, vol. 102, no. 52, pp. 10871–10878, 1998.

[24] I. Sosnowska, T. P. Neumaier, and E. Steichele, "Spiral magnetic ordering in bismuth ferrite," *Journal of Physics C: Solid State Physics*, vol. 15, no. 23, pp. 4835–4846, 1982.

[25] T.-J. Park, G. C. Papaefthymiou, A. J. Viescas, A. R. Moodenbaugh, and S. S. Wong, "Size-dependent magnetic properties of single-crystalline multiferroic $BiFeO_3$ nanoparticles," *Nano Letters*, vol. 7, no. 3, pp. 766–772, 2007.

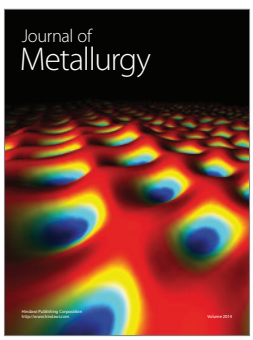

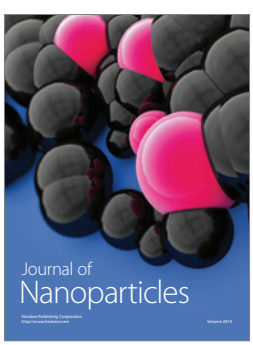

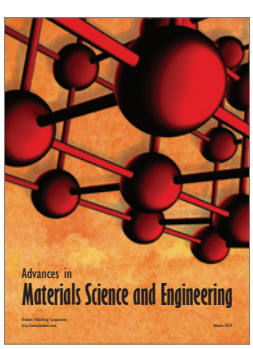

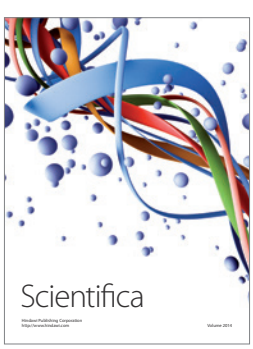

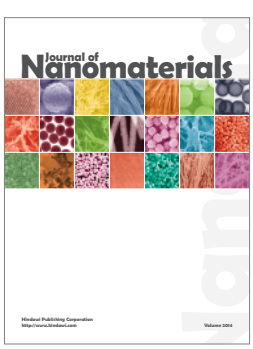

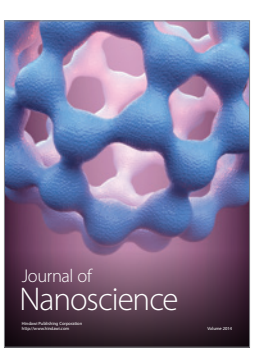

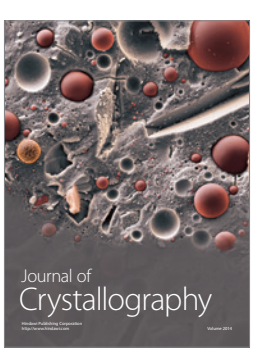

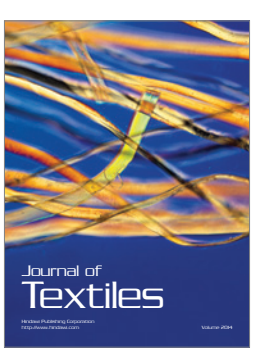

Hindawi

Submit your manuscripts at
http://www.hindawi.com